

Zebrafish *pax8* is required for otic placode induction and plays a redundant role with Pax2 genes in the maintenance of the otic placode

Melinda D. Mackereth^{1,*}, Su-Jin Kwak^{2,*}, Andreas Fritz¹ and Bruce B. Riley^{2,†}

¹Department of Biology, Emory University, Atlanta, GA 30322, USA

²Biology Department, Texas A&M University, College Station, TX 77843-3258, USA

*These authors contributed equally to this work

†Author for correspondence (e-mail: briley@mail.bio.tamu.edu)

Accepted 17 November 2004

Development 132, 371-382

Published by The Company of Biologists 2005

doi:10.1242/dev.01587

Summary

Vertebrate Pax2 and Pax8 proteins are closely related transcription factors hypothesized to regulate early aspects of inner ear development. In zebrafish and mouse, *Pax8* expression is the earliest known marker of otic induction, and *Pax2* homologs are expressed at slightly later stages of placodal development. Analysis of compound mutants has not been reported. To facilitate analysis of zebrafish *pax8*, we completed sequencing of the entire gene, including the 5' and 3' UTRs. *pax8* transcripts undergo complex alternative splicing to generate at least ten distinct isoforms. Two different subclasses of *pax8* splice isoforms encode different translation initiation sites. Antisense morpholinos (MOs) were designed to block translation from both start sites, and four additional MOs were designed to target different exon-intron boundaries to block splicing. Injection of MOs, individually and in various combinations, generated similar phenotypes. Otic induction was impaired, and otic vesicles were small. Regional ear markers were expressed correctly, but hair cell production was significantly reduced. This phenotype

was strongly enhanced by simultaneously disrupting either of the co-inducers *fgf3* or *fgf8*, or another early regulator, *dlx3b*, which is thought to act in a parallel pathway. In contrast, the phenotype caused by disrupting *foxi1*, which is required for *pax8* expression, was not enhanced by simultaneously disrupting *pax8*. Disrupting *pax8*, *pax2a* and *pax2b* did not further impair otic induction relative to loss of *pax8* alone. However, the amount of otic tissue gradually decreased in *pax8-pax2a-pax2b*-deficient embryos such that no otic tissue was detectable by 24 hours post-fertilization. Loss of otic tissue did not correlate with increased cell death, suggesting that otic cells dedifferentiate or redifferentiate as other cell type(s). These data show that *pax8* is initially required for normal otic induction, and subsequently *pax8*, *pax2a* and *pax2b* act redundantly to maintain otic fate.

Key words: Preplacodal domain, Otic placode, Genetic network, Paired, Fibroblast growth factor, *forkhead*, *distal-less*, *msxC*

Introduction

Pax proteins are key regulators of developmental processes including specification, differentiation, growth, survival, migration and morphogenesis (Chi and Epstein, 2002; Dahl et al., 1997; Mansouri et al., 1996; Stuart et al., 1994). Pax genes are present in organisms ranging from worms to mammals (Czerny et al., 1997; Dahl et al., 1997; Walther et al., 1991). Pax proteins are named for and defined by the presence of a highly conserved, N-terminal, 128-amino acid DNA-binding domain, the Paired domain (PD), which was first identified in the *Drosophila* pair-rule segmentation gene *paired* (Treisman et al., 1991). The PD consists of two subdomains that each bind DNA in adjacent major grooves of the helix (Xu et al., 1995). Several Pax proteins can also interact with DNA via a complete or partial homeodomain (Dahl et al., 1997; Stuart et al., 1994; Underhill and Gros, 1997). Transcriptional activity of Pax proteins is controlled by a C-terminal regulatory region containing both activating and inhibitory domains (Dorfler and Busslinger, 1996).

Extensive alternative splicing has been reported for many vertebrate Pax genes, including mammalian *Pax2*, *Pax3*, *Pax5*, *Pax6*, *Pax7* and *Pax8*, and zebrafish *pax2a*, *pax3*, *pax7*, and *pax9* (Barber et al., 1999; Barr et al., 1999; Epstein et al., 1994; Kozmik et al., 1997; Kozmik et al., 1993; Nornes et al., 1996; Puschel et al., 1992; Seo et al., 1998; Tavassoli et al., 1997; Vogan et al., 1996; Zwollo et al., 1997). Similarly, *Pax2/5/8* transcripts of the invertebrate chordate amphioxus (*Branchiostoma floridae*) are alternatively spliced (Krelova et al., 2002). In most cases, alternative splicing has been shown to produce protein isoforms with drastically different DNA binding specificities and transactivation potentials (Barber et al., 1999; Barr et al., 1999; Epstein et al., 1994; Kozmik et al., 1997; Kozmik et al., 1993; Nornes et al., 1996; Puschel et al., 1992; Seo et al., 1998; Tavassoli et al., 1997; Vogan et al., 1996; Zwollo et al., 1997). Thus, alternative splicing is a highly conserved means of increasing the functional repertoire of Pax genes.

The nine vertebrate Pax genes are grouped into four categories, with *Pax2/5/8* constituting one of these classes

(Pfeffer et al., 1998). This is an ancient group, with orthologs present in echinoderms, nematodes, and flies (Czerny et al., 1997). The sequences of the functional regions are nearly invariant among the vertebrate *Pax2/5/8* genes (Pfeffer et al., 1998). *Pax2/5/8* genes are expressed in a spatially and temporally overlapping manner at the midbrain-hindbrain junction and in the CNS; this expression pattern has been conserved from zebrafish to mouse (Pfeffer et al., 1998). *Pax2* and *Pax8* homologs are also expressed in the otic placode and pronephros in these species (Pfeffer et al., 1998; Plachov et al., 1990). Recent evidence has shown that *Pax2* and *Pax8* perform redundant functions during mammalian kidney development and are required for the earliest steps of this process (Bouchard et al., 2002; Mansouri et al., 1998). However, otic development in *Pax2/Pax8*-deficient mouse embryos has not yet been described. In both zebrafish and mouse, *Pax8* is strongly expressed in the primordium of the otic placode during late gastrulation, making it the earliest known marker of otic induction (Pfeffer et al., 1998). *Pax8* expression is maintained throughout placode development and is lost soon after formation of the otic vesicle (Pfeffer et al., 1998). *Pax2* homologs are expressed in the otic anlagen during early somitogenesis stages and are maintained in portions of the otic vesicle (Pfeffer et al., 1998). The *Pax8* knockout mouse does not show an otic phenotype (Bouchard et al., 2002; Mansouri et al., 1998), and the *Pax2* knockout mouse shows variable defects in derivatives of the medial otic vesicle where *Pax2* is expressed after the vesicle forms (Bouchard et al., 2000; Burton et al., 2004; Favor et al., 1996; Torres et al., 1996). The absence of an earlier or more severe phenotype may reflect redundancy between these genes. There are two *Pax2* homologs in zebrafish, *pax2a* and *pax2b*, and functional disruption of both genes reduces hair cell production but does not impair formation of the placode or vesicle (Whitfield et al., 2002). The extent to which *pax8* compensates for loss of *pax2a* and *pax2b* is not known.

Several upstream regulators of otic induction have been identified. The forkhead class transcription factor gene *foxi1* is expressed in the ventral ectoderm beginning at 50% epiboly. By mid-gastrulation *foxi1* expression is upregulated in the future otic placode prior to induction of *pax8*. Loss of *foxi1* prevents expression of *pax8* in the otic domain and severely compromises otic induction. Furthermore, misexpression of *foxi1* is sufficient to induce ectopic *pax8* (Nissen et al., 2003; Solomon et al., 2003). At least two other genes, *fgf3* and *fgf8*, are also necessary for *pax8* expression. These genes encode Fgf ligands that are expressed in the developing hindbrain between the prospective otic placodes. Loss of both *fgf* genes blocks otic induction, whereas misexpression of either gene is sufficient to induce ectopic otic tissue (Leger and Brand, 2002; Maroon et al., 2002; Phillips et al., 2001; Phillips et al., 2004). Thus, Fgf signaling and *foxi1* function converge to induce *pax8*, suggesting that *pax8* could be an important mediator of otic induction. In addition, zebrafish *dlx3b* and *dlx4b*, transcription factors with homeo-domains similar to *Drosophila distal-less* (Ekker et al., 1992a; Ellies et al., 1997), are required for otic placode formation. Combined loss of function of *dlx3b/4b* leads to a reduction or absence of otic placodes and *pax2a* expression in otic cells, but *pax8* expression initiates normally (Liu et al., 2003; Solomon and Fritz, 2002).

In this paper, we describe a role for *pax8* during otic

development. We have cloned full-length transcripts of zebrafish *pax8* and show that there are three main splice variants that encode proteins with different N-terminal sequences. Depletion of Pax8 function leads to compromised otic vesicle and inner ear morphology, and our data suggest that different isoforms have both overlapping and unique functions. We show a strong genetic interaction between *pax8* and *pax2a*, and to a lesser extent *pax2b*, implicating these genes in the maintenance of otic cell fate. Depletion of *pax8* enhances otic placode and vesicle defects in embryos with reduced Fgf signaling or in embryos that have been depleted for *dlx3b* function. In contrast, depletion of *pax8* does not enhance defects in embryos depleted for *foxi1*. These and other data support the hypothesis that *pax8* helps mediate otic induction downstream of *foxi1* and *fgf3* and *8* but in parallel with *dlx3b*. At later stages, *pax8* acts redundantly with Pax2 genes to maintain otic fate.

Materials and methods

Fish strains

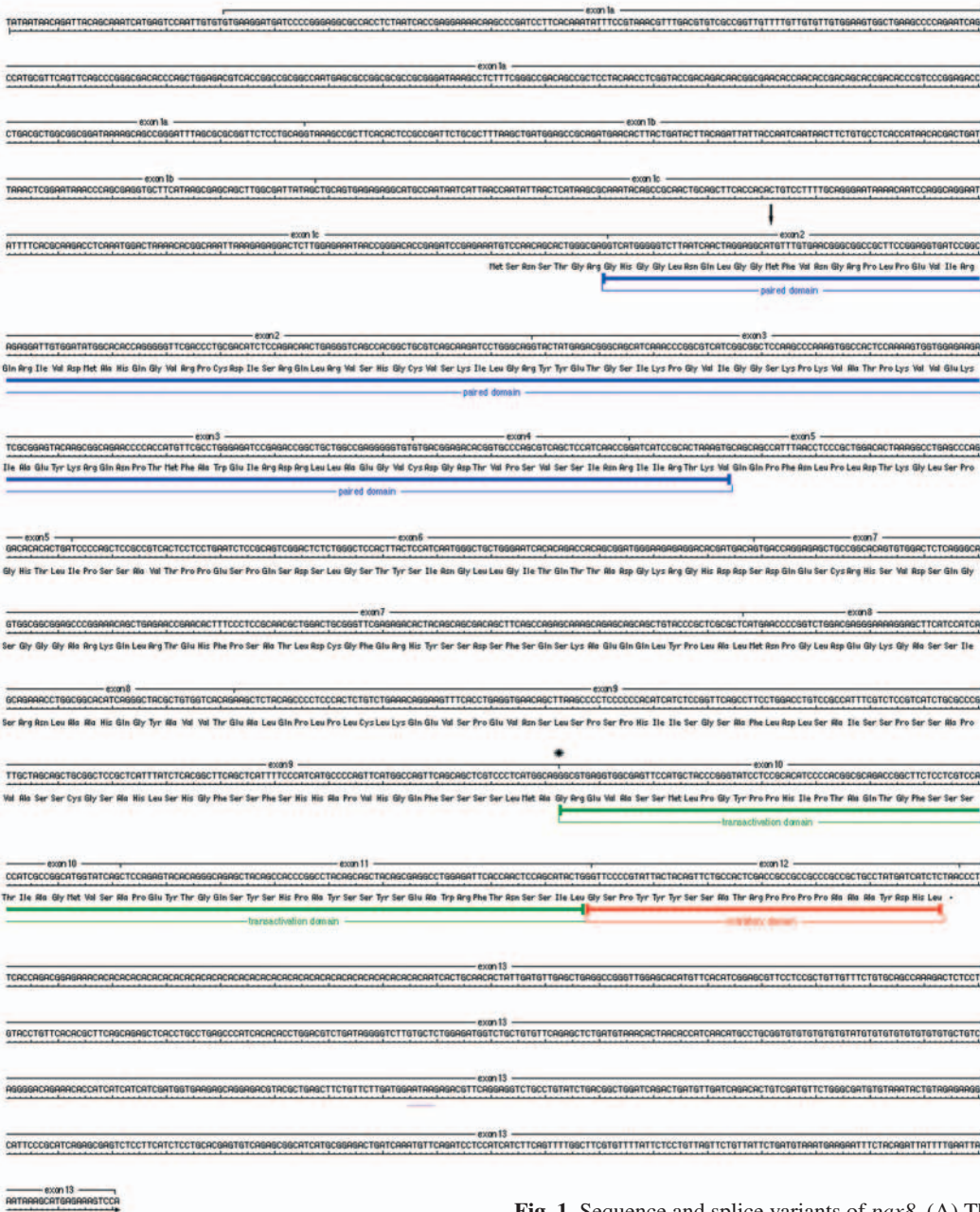
Embryos were developed at 28.5°C and staged according to standard criteria (Kimmel et al., 1995). Wild-type fish were derived from the AB line. *noi^{tu29a}* and *ace^{ti282a}* were derived from the Tu line (Brand et al., 1996) and used to assess functions of *pax2a* and *fgf8*, respectively. *noi^{tu29a}* is thought to be a null allele (Lun and Brand, 1998) whereas *ace^{ti282a}* is a strong hypomorph (Draper et al., 2001). Because *pax2a* and *fgf8* are closely linked, producing *ace-noi* double homozygotes required that we first produce a recombinant line in which both mutant loci reside on the same chromosome. The rate of recombination between *fgf8* and *pax2a* is roughly 1.5%, so nearly 25% of intercross progeny produced in this line are double homozygotes.

pax8 5' and 3' RACE cloning and sequencing

RNA was isolated from 3-5 somite and 24-hour embryos using TRIPURE reagent (Roche). For the 5' RACE reaction, 3-5 somite stage RNA was processed using the First Choice RLM-RACE kit from Ambion. cDNA was synthesized using a *pax8*-specific primer (CAGCGCCGCGGAGGGAAAGT) and C. therm polymerase (Roche) at 68°C for reverse transcription. Subsequently, PCR was performed using a second, nested *pax8*-specific primer (GCGGCGGTCGATTGGCAAACTGTA) and the 5' RACE adaptor outer primer (Ambion). A fraction of this reaction was used as template in a second PCR amplification with a third, nested *pax8*-specific primer (AACGGGCGCAGATGACGGAGACGAA) and the 5' RACE adaptor inner primer. All PCRs were performed using the Clontech Advantage-GC2 protocol with a final concentration of 1 M GC-melt. The resulting amplification products were cloned into pCRII Topo vector (Invitrogen) and sequenced. The 24-hour RNA was reverse transcribed using the CDS primer from the SMART II kit (Clontech) and C. Therm polymerase. 3' RACE was performed using a *pax8*-specific primer (CATCAATGGGCTGCTGGGAATCA) and the CDS primer (Clontech) in an initial PCR. A fraction of this reaction was used for a second PCR amplification with a nested *pax8*-specific primer (TCCGAGGGCTGAGGTATTTGTC) and the PCR primer supplied in the Clontech SMART II kit. A third round of PCR was performed using a fraction of the second PCR reaction as template and the *pax8*-specific primer (GCCAGTTC-AGCAGCCCGTCCCTCAT) and the PCR primer (Clontech). The resulting products were cloned into the pCRII Topo vector and sequenced.

For the splice variant analysis, *pax8*-specific primers located in the 5' UTR [exon 1a (Fig. 1A); GACAGACAACGGCGAACACCAA-CAC] and the 3'UTR [exon 13 (Fig. 1A); ACCCGGCCTCAG-

A



B

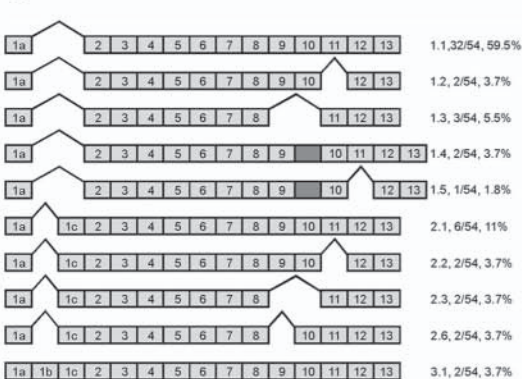


Fig. 1. Sequence and splice variants of *pax8*. (A) The complete sequence of the *pax8* variant 3 transcript. Exons predicted by comparison to genomic sequence are indicated above the sequence. The transcription start site, preceded by a TATAA box, begins with exon 1a. Exon 1 is contiguous with genomic DNA sequence, but has been subdivided into exons 1a, 1b, and 1c to indicate that the splice variants shown in Fig. 1B contain different parts of exon 1. The arrow indicates the putative start codon used in variant 1 transcripts. The star indicates that some transcripts use an alternate splice donor site that extends exon 9 by 33 bp (sequence not shown). The canonical Paired domain and predicted transactivation and inhibitory domains are indicated below the sequence. Polyadenylation (polyA) sites are underlined in purple; the majority of transcripts (52/54) use the first polyA site. (B) A schematic representation (not to scale) of the splice variants observed in *pax8* transcripts. The variant name (e.g. 1.1, 1.2), total number of representative transcripts out of 54 total sequenced, and percentage abundance are indicated after each schematic transcript. The unlabeled box between exon 9 and exon 10 in variants 1.4 and 1.5 indicates an additional 11 amino acid insert (see also Fig. 1A) resulting from the use of an alternate splice donor site. The predicted coding sequence for variants 2 and 3 begins with the start codon in exon 1c; all variant 1 transcripts use the start codon in exon 2 indicated by the arrow in Fig. 1A.

CTCAACATCAATAG] were used to amplify *pax8* transcripts from 24-hour cDNA (described above), using the Advantage-GC2 PCR protocol with a 1 M concentration of GC-melt. The resulting products were cloned into the pCRII Topo vector and sequenced.

Morpholino injections

Morpholino oligomers obtained from Gene Tools Inc. were diluted and injected as previously described (Nasevicius and Ekker, 2000; Phillips et al., 2001). A total of 1–5 ng MO was injected per embryo. At least 25 specimens were examined for each experiment.

To knockdown *pax8*, translation-blocking morpholinos and splice-blocking morpholinos were generated as follows: translation blocker for splice variant 1 (variant 1 MO): 5' GTTCACAAACATGCCTCC-TAGTTGA 3'; translation blocker for splice variants 2 and 3 (variant 2/3 MO): 5' GACCTCGCCAGTGCTGTTGGACAT 3'; splice blocker exon6/7 (splice donor site): 5' CTGCACTACTGT-CATCGTGCCTC 3'; splice blocker exon6/7 (splice acceptor site): 5' CAGCTCTCCTGGTCACTGCACAAC 3'; splice blocker exon3 (paired domain): 5' GTAGCGGTGACACACCCCTCGGCC 3'; splice blocker exon7/8 (homeo domain): 5' TGCGGTGTTCTGCAC-CTGCTCTGCT 3'. Unless stated otherwise, *pax8* morphants were injected with 2.5 ng each of variant 1 MO and variant 2/3 MO to maximally disrupt *pax8* function.

To knockdown *fgf3*, two translation-blocking sequences were co-injected: *fgf3*-MO #1, 5' CATTGTGGCATCGCGGGATGTCCGC 3'; *fgf3*-MO #2, 5' GGTCCCATCAAAGAAGTATCATTTG 3'. Other morpholino sequences used were as follows: *dlx3b*-MO translation blocker, 5' ATATGTCGGTCCACTCATCCTTTAAT 3'; *foxi1*-MO translation blocker, 5' TAATCCGCTCTCCCTCCAGAAA 3'; *pax2b*-MO translation blocker: 5' GGTCTGCCTTACAGTGAATATCCAT 3'.

Immunofluorescent staining

Embryos were raised in 0.3% PTU solution to inhibit the formation of melanocytes. Embryos were fixed and stained as previously described (Riley et al., 1999) using polyclonal anti-mouse Pax2 antibody (Berkeley Antibody company, 1:100 dilution) and monoclonal anti-acetylated tubulin antibody (Sigma T-6793, 1:100). Alexa 546 goat anti-rabbit IgG (Molecular Probes A-11010, 1:50) and Alexa 488 goat anti-mouse IgG (Molecular Probes A-11001, 1:50) were used as secondary antibodies.

In situ hybridization

In situ hybridization was carried out as described in Phillips et al. (Phillips et al., 2001), and two-color staining was performed as described by Jowett (Jowett, 1996) with minor modifications. Antisense riboprobes were transcribed from plasmids containing the following: *dlx3b* (Ekker et al., 1992a); *krox20* (Oxtoby and Jowett, 1993); *msxC* (Ekker et al., 1992b); *pax2a* (Krauss et al., 1991); *pax5* and *pax8* (Pfeffer et al., 1998).

Results

Pax8 transcript structure

The previously published sequence for zebrafish *pax8* was incomplete, lacking 3' UTR sequences and 5' sequences, including the putative start codon (Pfeffer et al., 1998). In order to facilitate design of translation-blocking morpholinos, complete *pax8* cDNAs were generated using RACE by RT-PCR on adaptor ligated mRNA from 3–5 somite stage and 24-hour embryos. Sequence analysis of the 5' RACE clones indicated that *pax8* is alternatively spliced, resulting in two different predicted start codons (Fig. 1A). Because members of the Pax gene family are subject to alternative splicing (Barber et al., 1999; Barr et al., 1999; Epstein et al., 1994; Kozmik et

al., 1997; Kozmik et al., 1993; Nornes et al., 1996; Puschel et al., 1992; Seo et al., 1998; Tavassoli et al., 1997; Vogan et al., 1996; Zwollo et al., 1997), primers in the predicted 5' UTR and 3' UTR were designed and RT-PCR was performed to obtain a collection of clones containing *pax8* transcripts with a complete coding sequence. A total of 54 clones were randomly selected and sequenced, and the results of this analysis are summarized in Fig. 1B. To verify these results, the cDNA sequences were used to search the genome assembly database (assembly Zv2; http://www.sanger.ac.uk/Projects/D_zebrafish/). Based on this comparison and the previously available data, the zebrafish *pax8* gene consists of at least 13 exons, and we have renumbered them accordingly (Fig. 1A). The predominant class of transcripts (32/54, 59.5%; Fig. 1B) is variant 1.1, which contains exon 1a, then exon 2 and all subsequent exons. The predicted ORF for variant 1 starts ten amino acids within the canonical Paired domain and is contiguous with the previously published sequence. Interestingly, *Fugu pax8* also encodes a methionine at position 10 of the Paired domain (Pfeffer et al., 1998), and thus may encode a similar set of Pax8 proteins as zebrafish. The second most frequent class of transcripts (6/54, 11%; Fig. 1B) is variant 2.1, which contains exon 1a, exon 1c, and then exon 2 and all following exons. Exon 1c provides an alternate potential start codon, leading to a predicted protein that starts eight amino acids N-terminal to the canonical Paired domain (Fig. 1A). Variant 3 transcripts appear to be rare (2/54, 4% of our clones) and encode the same predicted protein sequence as variant 2 transcripts.

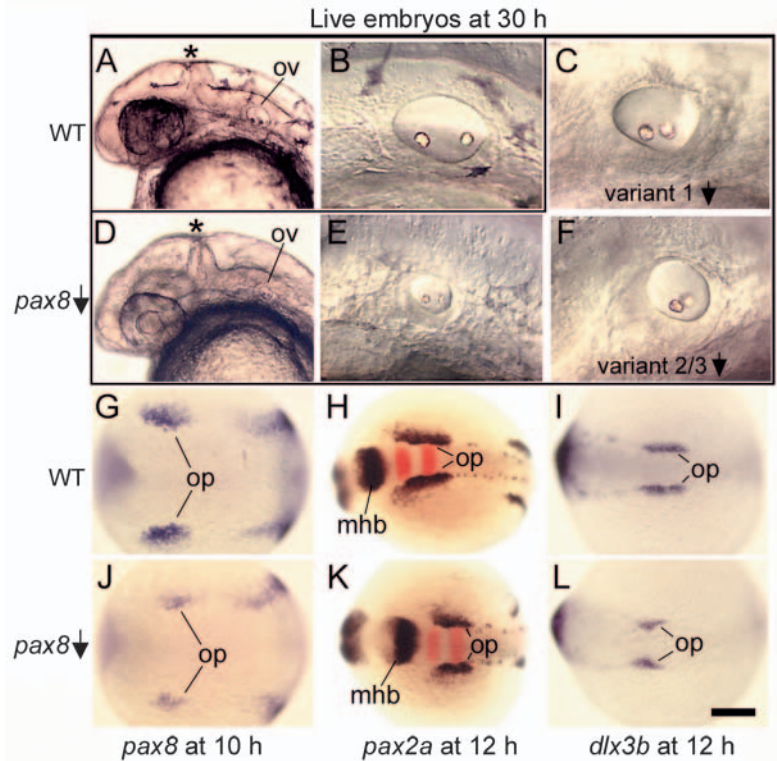
Variants 1.2 (3.7%) and 2.2 (3.7%) lack exon 11, which encodes a portion of the transactivation domain. Similarly, variants 1.3 (5.5%) and 2.3 (3.7%) lack exons 9 and 10, which also encode part of the transactivation domain. Variants 1.4 (3.7%) and 1.5 (1.8%) use an alternate splice donor site, leading to an insert between exons 9 and 10; this insert is in frame and would add 11 amino acids to the transactivation domain (not shown in Fig. 1A sequence). In addition to the insert, variant 1.5 also lacks exon 11. Variant 2.6 lacks part of the transactivation domain due to the absence of exon 9.

The sequence analysis shows that *pax8* transcripts are subject to extensive alternative splicing. To address the potential functional significance of different Pax8 isoforms, artificial mRNA for variants 1.1 or 2.1 (full length) and 1.3 or 2.3 (nonfunctional transactivation domain) were injected into one-cell embryos. Ectopic overexpression of either full length variant leads to severe gastrulation defects, precluding a meaningful interpretation of *pax8* function in otic placode formation. Conversely, injection of the isoforms lacking the transactivation domain did not lead to any detectable phenotypes in otic placode or vesicle morphology (data not shown).

Functional analysis of *pax8*

We designed morpholino oligonucleotides (MO) to knock down *pax8* function. Four MOs were designed to block pre-mRNA splicing at distinct splice junction sites (Draper et al., 2001), and two additional MOs were designed to target the sequence around each of the predicted start codons (Nasevicius and Ekker, 2000). Together, these two MOs are predicted to block translation of all isoforms (Fig. 1A). Co-injection of the translation-blocking MOs resulted in the most consistent and reproducible phenotypes, and this approach was used in all

Fig. 2. Assessment of Pax8 function in otic induction. (A,D) Head region of live wild-type (A) and *pax8*-MO injected (D) embryos at 30 hpf. The *pax8*-MO-injected embryo has a narrow midbrain-hindbrain border (asterisk), and small otic vesicles (ov). (B,E) Otic vesicles at 30 hpf in live wild-type (B) and *pax8*-MO-injected (E) embryos. (C,F) Otic vesicles at 30 hpf in embryos injected with v1-MO to knockdown variant 1 isoforms of *pax8* (C) or v2/3-MO to knockdown variant 2 and 3 isoforms of *pax8* (F). (G,J) *pax8* expression at 10 hpf in wild-type (G) and *pax8*-MO-injected (J) embryos. (H,K) Expression of *pax2a* (blue) and *krox20* (red) at 12 hpf in wild-type (H) and *pax8*-MO-injected (K) embryos. (I,L) *dlx3b* expression at 12 hpf in wild-type (I) and *pax8*-MO-injected (L) embryos. Images show lateral views with anterior to the left and dorsal to the top (A-F); or dorsal views with anterior to the left (G-L). mhb, midbrain-hindbrain border; op, otic placode; ov, otic vesicle. Scale bar in L: 200 μ m for H,K; 170 μ m for G,I,J,L; 150 μ m for A,D; 40 μ m for B,C,E,F.



subsequent studies. Co-injection of the two translation blockers plus two of the four splice-blocking MOs did not produce any additional phenotypic defects, although nonspecific necrosis was seen at higher MO concentrations (not shown), further suggesting that the translation-blocking MOs effectively block *pax8* function.

At 24 hpf, reduction of *pax8* translation in embryos injected with both translation-blocking *pax8* MOs (*pax8* morphants) causes a slightly shortened trunk/tail axis and a reduced midbrain-hindbrain border with mild necrosis in adjacent brain tissue (Fig. 2A,D). Furthermore, the otic vesicle is reduced in its linear dimensions by roughly half (Fig. 2B,E). These phenotypic changes are observed in over 90% of *pax8* morphants. Embryos injected with only variant 1 MO (Fig. 2C) or variant 2/3 MO (Fig. 2F) display an otic vesicle phenotype of intermediate severity, with the variant 2/3 morphant embryos showing a slightly more affected otic vesicle. Because *pax8* is one of the earliest known markers of preotic development (Pfeffer et al., 1998), we analyzed the initial stages of otic induction in *pax8* morphants. Knockdown of *pax8* does not eliminate *pax8* mRNA expression in otic precursor cells, but reduces the size of the preotic domain of *pax8* expression at all stages examined (Fig. 2G,J). The level of *pax8* expression in these cells is also reduced, suggesting a certain degree of autoregulation. Two other preotic markers, *pax2a* and *dlx3b*, also display reduced preotic domains, but levels of expression are relatively normal (Fig. 2H,K,I,L). Hindbrain (HB) patterning is normal in *pax8* morphants as judged by expression patterns of *krox20*, *fgf3*, *fgf8*, *wnt8* and *wnt8b* (Fig. 2H,K; see also Fig. 5), suggesting that impairment of preotic development is not due to loss of HB signals. We infer that a reduced level of *pax8* impairs the response of preplacodal cells to otic-inducing signals (see Discussion). Alternatively, otic induction may proceed normally in *pax8* morphants, but placodal cells proliferate less in the absence of Pax8. However, previously published work on the role of Fgf3 and Fgf10 during otic development in the mouse suggests that this latter explanation is not the case (Alvarez et al., 2003; Wright and Mansour, 2003).

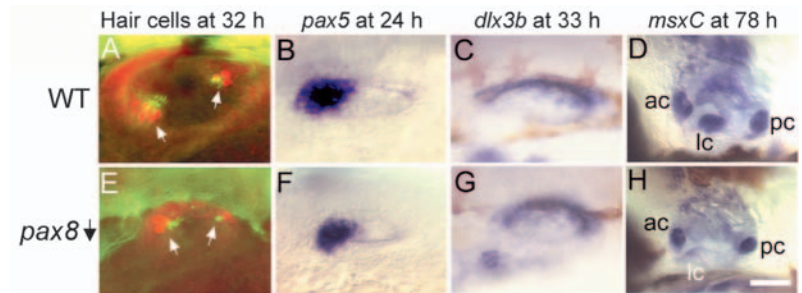
We also examined later aspects of otic patterning in *pax8*

morphants. General features of anterior-posterior, dorso-ventral and medio-lateral patterning appear unaffected, as shown by normal expression of *pax5* in the anterior (Fig. 3B,F), *dlx3b* in the dorsal (Fig. 3C,G), and *pax2a* in the ventromedial portions of the otic vesicle (Fig. 3A,E). However, hair cell production is reduced by an average of $42 \pm 11\%$ ($n=59$; compare Fig. 3A and E), and severely affected specimens produce only a single macula per ear (not shown). Cristae typically form by 72 hpf and express *msxC*, although the level of expression is usually reduced in the lateral crista (Fig. 3D,H). In severely affected specimens with very small otic vesicles, one or more cristae are fused or missing (not shown). Later stages of otic development become increasingly aberrant as embryos begin to degenerate and die (not shown). Since *pax8* is not expressed in the ear past 19 hpf, reduction in the vesicle and sensory epithelia presumably arise from earlier deficits in the placode or preplacode resulting from reduced levels of *pax8*.

Interactions between *pax8* and Fgf genes

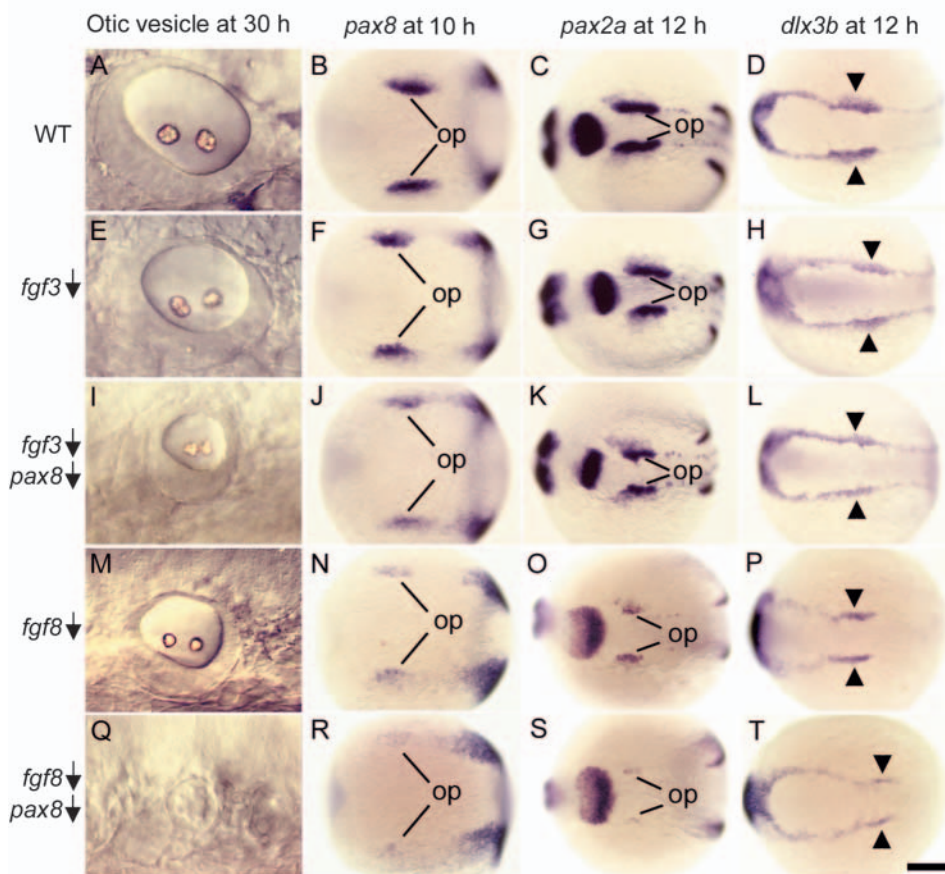
Fgf signaling appears to be the principal inducer of otic development in all vertebrates (Noramly and Grainger, 2002; Riley and Phillips, 2003). In zebrafish, *fgf3* and *fgf8* are expressed in periotic tissues during gastrulation and are essential for otic induction (Leger and Brand, 2002; Maroon et al., 2002; Phillips et al., 2001). Furthermore, in the experimental context of the whole embryo, misexpression of *fgf3* or *fgf8* can lead to the formation of ectopic otic placodes (Phillips et al., 2004). Induction of *pax8* expression is the earliest response to Fgf signaling and does not occur in the absence of Fgf signaling. We hypothesized that *pax8* helps mediate otic induction or early differentiation in response to Fgf signaling. In support of this hypothesis, the phenotype

Fig. 3. Assessment of Pax8 function in otic vesicle patterning. (A,E) Otic vesicles at 32 hpf stained with anti-Pax2 (red) and anti-acetylated tubulin (green) antibodies to label hair cells (Riley et al., 1999) in wild-type (A) and *pax8*-MO-injected (E) embryos. Hair cell patches are indicated (white arrows). Injected embryos produce fewer hair cells than normal. In the experiment shown here, an average of 5.2 ± 1.1 hair cells were seen in *pax8* morphants ($n=59$ ears), compared to 9.2 ± 1.4 hair cells in wild type embryos ($n=10$ ears); 5-10% of *pax8* morphants produce only one macula per ear (not shown). (B,F) *pax5* expression at 24 hpf in wild-type (B) and *pax8*-MO-injected (F) embryos. (C,G) *dlx3b* expression at 33 hpf in wild-type (C) and *pax8*-MO-injected (G) embryos. (D,H) *msxC* expression marks developing cristae in the otic vesicle at 78 hpf in wild-type (D) and *pax8*-MO-injected (H) embryos. The lateral crista is present in the injected embryo but shows strongly reduced expression of *msxC*. Defects in development of cristae and semicircular canals are highly variable in *pax8* morphants. Images show lateral views with anterior to the left and dorsal to the top. ac, anterior crista; lc, lateral crista; pc, posterior crista. Scale bar in H: 90 μ m for D,H, 40 μ m for C,G, and 30 μ m for A,B,E,F.



observed in *pax8* morphants (Figs 2 and 3) resembles that observed in embryos disrupted for either *fgf3* or *fgf8* (Fig. 4E,M). We tested this relationship further by examining the effects of disrupting *pax8* and either *fgf3* or *fgf8*. Because *fgf3* and *fgf8* are partially redundant, blocking either function alone causes only moderate reduction in the expression domains of preotic markers *pax8*, *pax2a*, and *dlx3b* (Fig. 4F-H,N-P), with corresponding reduction in the size of the otic vesicle (Fig. 4E,M). These tissues are further reduced in embryos depleted for both *pax8* and *fgf3* (Fig. 4I-L). Depleting *pax8* in *ace* (*fgf8*) mutants causes even more severe deficiencies in otic development: at early stages, expression domains of *pax8* and *pax2a* are strongly reduced, upregulation of *dlx3b* does not

occur, and at later stages the otic vesicle is rudimentary and produces no hair cells or otoliths (Fig. 4Q-T). It is unclear whether the stronger interaction of *pax8* with *fgf8* compared to *fgf3* reflects functional differences between these ligands or differing degrees of functional disruption. A recent report suggests that *fgf8* plays a more dominant role than *fgf3* in early hindbrain patterning (Wiellette and Sive, 2004), and may thus also have a more pronounced role in otic induction. In either case, the above data are consistent with the hypothesis that *pax8* helps mediate the effects of both Fgfs. The fact that otic development is not totally ablated is consistent with the notion that *pax8* is not the only gene involved in the early response to Fgf signaling.



Interactions between *pax8* and Pax2 genes

Two other Pax genes are coexpressed with *pax8* in preotic cells, albeit at slightly later stages: *pax2a* is expressed in the otic anlagen by 11 hpf (3 somites) and *pax2b* is expressed by 13.5 hpf (9 somites) (Pfeffer et al., 1998). As closely allied members of the

Fig. 4. Interaction of *pax8* with *fgf3* and *fgf8*. Wild-type embryos (A-D), wild-type embryos injected with *fgf3*-MO (E-H), wild-type embryos co-injected with *fgf3*-MO and *pax8*-MO (I-L), *ace* (*fgf8*) mutants (M-P), and *ace* mutants injected with *pax8*-MO (Q-T). Images show lateral views of the otic vesicle at 30 hpf (A,E,I,M,Q), and dorsal views of *pax8* expression at 10 hpf (B,F,J,N,R), *pax2a* expression at 12 hpf (C,G,K,O,S) and *dlx3b* expression at 12 hpf (D,H,L,P,T). op, otic placode. Arrowheads mark the otic region where *dlx3b* expression normally shows marked upregulation. Anterior is to the left in all specimens. Op, otic placode. Scale bar in T: 30 μ m for A,E,I,M; 200 μ m for B-D,F-H,J-L,N-P,R-T.

pax2/5/8 family, these three genes could provide multiple levels of redundancy during otic development. Notably, embryos deficient in both *pax2a* and *pax2b* produce relative normal otic vesicles, with defects being limited to reduced hair cell production (Whitfield et al., 2002). This surprisingly mild phenotype possibly reflects compensation by *pax8*. Similarly, later expression of *pax2a* and *pax2b* could ameliorate the effects of disrupting *pax8* function. To address these possibilities, we injected *pax8*-MO and *pax2b*-MO into *noi* (*pax2a*) mutants (Fig. 5A'-D'). Early placode development in *pax2a-pax2b-pax8*-deficient embryos is similar to that in *pax8* morphants. However, by 18 hpf, the otic domain of *pax2a* is

severely reduced in *pax2a-pax2b-pax8*-deficient embryos (Fig. 5B'). By 24 hpf, the otic domain of *pax2a* is lost entirely in about half of *pax2a-pax2b-pax8*-deficient embryos (47%, $n=36$; Fig. 5C'), and there are no morphological signs of otic development (Fig. 5D'). Staining with acridine orange indicates that there is no noticeable increase in cell death in the periotic region (not shown), suggesting that otic cells dedifferentiate in the absence of *pax2/8* function. In agreement, about half of *pax2a-pax2b-pax8*-deficient embryos show diffuse expression of *dlx3b* in the otic region or no otic expression at all (11/30 and 3/30, respectively, Fig. 5E',F'). In addition, a scattering of *dlx3b*-expressing cells appears

Fig. 5. Relative functions of *pax8*, *pax2a* and *pax2b*. (A-C) *pax2a* expression in wild-type embryos at 14 hpf (A), 18 hpf (B) and 24 hpf (C). (D) Head region of an uninjected *noi* (*pax2a*) mutant at 30 hpf. The otic vesicle has essentially normal morphology. A'-D', *noi* (*pax2a*) mutants co-injected with *pax8*-MO and *pax2b*-MO showing *pax2a* expression at 14 hpf (A'), 18 hpf (B') and 24 hpf (C'), and a live specimen with no otic vesicles at 30 hpf (D'). *krox20* expression in the hindbrain is shown in red (B,B'). (E,E',F,F') *dlx3b* expression at 24 hpf in a wild-type embryo (E), a wild-type embryo injected with *pax8*-MO (F), and *noi* (*pax2a*) mutants co-injected with *pax8*-MO and *pax2b*-MO (E',F'). The specimen in E' lacks morphological otic vesicles but does show a scattering of *dlx3b*-expressing cells in the otic region (asterisk). The specimen in F' lacks morphological signs of otic development and also shows no *dlx3b* expression in the otic region (asterisk). G,G',H,H', *fgf3* expression in wild-type embryos at 14 hpf (G) and 19 hpf (H) and in *pax2a-pax2b-pax8*-deficient embryos at 14 hpf (G') and 19 hpf (H'). Expression in the hindbrain (r4) is normal in all specimens, whereas expression in the otic vesicle (ov) is strongly reduced at 19 hpf in *pax2a-pax2b-pax8*-deficient embryos (compare H,H'). (I,I') *sox9a* expression at 13.5 hpf in wild-type (I) and *pax2a-pax2b-pax8*-deficient (I') embryos. (J-L,J'-L') claudinA expression in wild-type embryos at 13.5 hpf (J) and 24 hpf (K,L), and in *pax2a-pax2b-pax8*-deficient embryos at 13.5 hpf (J') and 24 hpf (K',L'). M-P, wild-type embryos co-injected with *pax8*-MO and *pax2b*-MO showing expression of *pax2a* at 14 hpf (M) and 18 hpf (N), the head region of a live specimen with a small otic vesicle at 30 hpf (O), and an enlargement of the otic vesicle of the same specimen (P). Images show dorsal views with anterior to the left (A,A',G-J,G'-J',M), dorsal views with anterior to the top (B,B',C,C',K,K',N), or lateral views with anterior to the left (D-F,D'-F',L,L',O,P). a, pharyngeal arches; asterisk, region where otic vesicle normally forms; mhb, midbrain-hindbrain border; op, otic placode; ov, otic vesicle; r4, rhombomere 4 of the hindbrain. Scale bar in P: 170 μ m for A,A',G,G',I,I',J',J',M; 75 μ m for B-F,B'-F',H,H',K,L,K',L',N,O; 19 μ m for P.

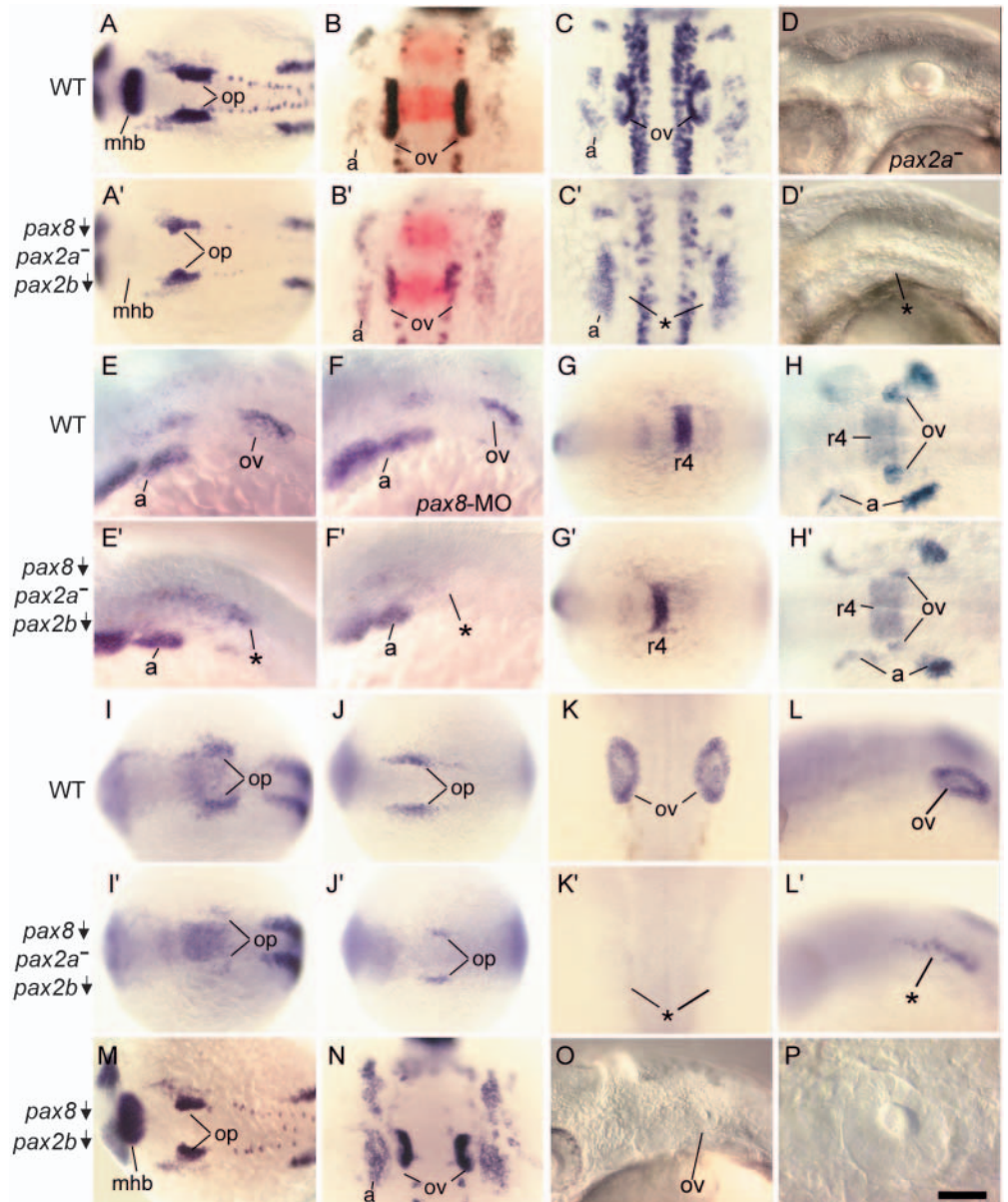
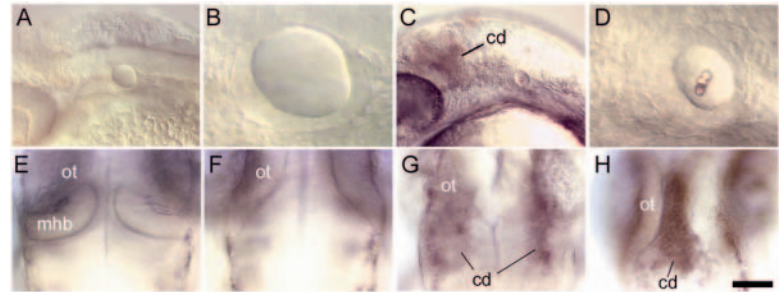


Fig. 6. Distinct functions of *pax8* splice isoforms. (A–D) Lateral views of the head and otic structures at 30 hpf in *noi* (*pax2a*) mutants injected either with *pax8* variant 1 MO (A,B) or *noi* mutants injected with *pax8* variant 2/3 MO (C,D). Most *noi* mutants knocked down for variant 1 isoforms produce a moderate-sized otic vesicle containing hair cells but lacking otoliths (B). In contrast, *noi* mutants knocked down for variant 2 and 3 isoforms typically produce a small otic vesicle containing both hair cells and otoliths (D) or no otic vesicle at all (data not shown). In addition, all *noi* mutants knocked down for variant 2 and 3 isoforms show persistent cell death (cd) in the midbrain-hindbrain region. (E–H) Dorsal views of the midbrain-hindbrain border region at 30 hpf in an uninjected wild-type embryo (E), an uninjected *noi* mutant (F), a *noi* mutant injected with *pax8* variant 1 MO (G) and a *noi* mutant injected with *pax8* variant 2/3 MO (H). Increased cell death is not evident in the majority of *noi* mutants knocked down for variant 1 isoforms (A) and, if present (G), cell death is diffuse and limited to dorsolateral tissue. In *noi* mutants knocked down for variant 2 and 3 isoforms, cell death is invariably present, intense, and localized to the midline of the midbrain-hindbrain border region (H). Anterior is to the left (A–D) or to the top (E–F). cd, cell death; mhb, midbrain-hindbrain border; ot, optic tectum. Scale bar in H: 75 μ m for A,C; 50 μ m for E–H; 19 μ m for B,D.



between the otic territory and pharyngeal arches, a region normally devoid of *dlx3b* expression. It is possible that these ectopic *dlx3b*-expressing cells are the dispersed remnants of the otic vesicle. Expression of other otic markers shows similar results. For example, *sox9a* expression is initially induced but is barely detectable in *pax2a-pax2b-pax8*-deficient embryos by 13.5 hpf (Fig. 5I,I'). *claudinA* is expressed in a reduced otic domain at 13.5 hpf. By 24 hpf, about half of *pax2a-pax2b-pax8*-deficient embryos show either no *claudinA* expression (9/25, Fig. 5K') or a diffuse scattering of expressing cells, again suggesting dispersal of otic remnants (5/25, Fig. 5L'). In summary, otic induction appears no worse in *pax2a-pax2b-pax8*-deficient embryos than in *pax8* morphants, but the otic placode is not maintained properly at later stages. Various hindbrain markers including *krox20*, *fgf3*, *fgf8*, *wnt8*, and *wnt8b* (Fig. 5B',G',H', and data not shown) are induced and maintained normally, suggesting that the failure to maintain otic fate is not due to loss of hindbrain signaling.

A similar phenotype to the *pax2a-pax2b-pax8*-deficient phenotype is seen in *noi* (*pax2a*)-*pax8*-deficient embryos (not shown). Because *pax2b* is still expressed, we infer that *pax2b* alone is not sufficient to maintain otic development. Nevertheless, the frequency of total ear loss in *noi* (*pax2a*)-

pax8-deficient embryos (22%, $n=23$) is lower than in *pax2a-pax2b-pax8*-deficient embryos (47%, $n=36$), suggesting that *pax2b* can contribute to otic maintenance. To test this further, we injected wild-type embryos with *pax2b*-MO and *pax8*-MO. Otic development is similar to that seen in *pax8*-deficient embryos through 18 hpf (Fig. 5M,N, and data not shown). However, *pax2b-pax8*-deficient embryos produce a much smaller otic vesicle than *pax8*-deficient embryos and usually lacks otoliths (Fig. 5O,P), suggesting significant loss of otic tissue after the vesicle begins to form. Thus, both *pax2a* and *pax2b* play a role in otic maintenance, but the requirement for *pax2a* appears more critical.

Because of the strong interaction between *pax8* and *pax2a*, we used the *noi* (*pax2a*) mutation to provide a sensitized background in which to test the relative roles of different *pax8* splice variants. *pax8* variant 1 MO blocks translation of variant 1 isoforms, which lack the N-terminal Paired domain, whereas *pax8* variant 2/3 MO blocks translation of isoforms predicted to include the entire Paired domain. Injection of *pax8* variant 1 MO into *noi* (*pax2a*) mutants usually results in production of a moderately reduced otic vesicle containing hair cells but no otoliths (83%, $n=84$, Fig. 6A,B). In contrast, injection of *pax8* variant 2/3 MO into *noi* (*pax2a*) mutants ablates the ear entirely (21/76) or results in production of a relatively small otic vesicle (55/76). In the latter case, however, otoliths are usually produced (Fig. 6C,D). The two translation blockers also differentially affect brain development in the region of the midbrain-hindbrain border (MHB). The MHB does not form in *noi* (*pax2a*) mutants. Mutants injected with *pax8* variant 2/3 MO invariably show a persistent and intense band of cell death localized to the ventral midline of the MHB region (Fig. 6C,H). This pattern of cell death is never

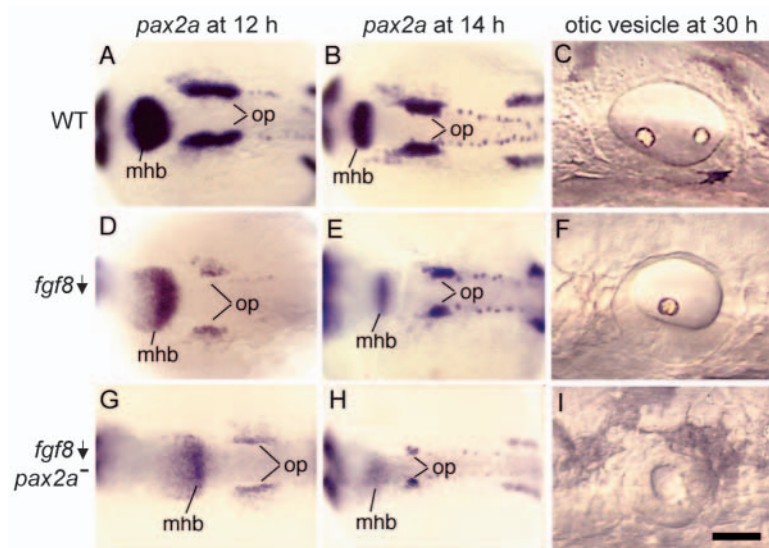


Fig. 7. *pax2a* interacts with *fgf8*. Wild-type embryos (A–C), *ace* (*fgf8*) single mutants (D–F) and *ace-noi* (*fgf8-pax2a*) double mutants (G–I). Images show dorsal views of *pax2a* expression at 12 hpf (A,D,G) and 14 hpf (B,E,H), and lateral views of otic vesicles at 30 hpf (C,F,I). The specimen in B is the same as in Fig. 5A, and the specimen in C is the same as in Fig. 2B. Anterior is to the left in all specimens. mhb, midbrain-hindbrain border; op, otic placode. Scale bar in I: 170 μ m for A,B,D,E,G,H; 35 μ m for C,F,I.

observed in uninjected *noi* (*pax2a*) mutants nor in mutants injected with *pax8* variant 1 MO (Fig. 6A,F). Instead, 20–30% of *noi* (*pax2a*) mutants injected with *pax8* variant 1 MO show a moderate increase in cell death in the dorsolateral MHB region (Fig. 6G). The significance of these differences is unclear at present, but the data strongly suggest that Pax8 isoforms containing a complete vs. partial Paired domain have at least some distinct developmental functions.

Interactions between *pax2a* and Fgf genes

A role for Pax2 genes in placode maintenance has not been previously reported, so this function was further investigated by analyzing the interaction between *fgf* genes and *pax2a*. In *ace-noi* (*fgf8-pax2a*) double mutants, expression of preotic markers is initially comparable to that seen in *ace* single mutants. However, the otic domain of *pax2a* shrinks dramatically in *ace-noi* double mutants such that, by 14 hpf, it is much smaller than in either *ace* or *noi* single mutants (Fig. 7D,E,G,H). *ace-noi* double mutants produce only very small otic vesicles containing few hair cells and no otoliths (Fig. 7I; and data not shown). In severely affected specimens, otic vesicles are so small that they can only be detected at high magnification using DIC optics. Similar results are obtained when *fgf3* is knocked down in *noi* (*pax2a*) mutants (not shown). Presumably, Fgf depletion impairs early preotic development such that *pax2a* function becomes critical for this process. When *pax2a* is disrupted in addition to *fgf3* or *fgf8*, the majority of placodal cells are unable to maintain otic fate.

Pax8 interaction with other transcription factors, Foxi1 and Dlx3b

foxi1 is one of the earliest regulators of preotic development identified (Nissen et al., 2003; Solomon et al., 2003). Loss of *foxi1* causes a severe phenotype characterized by production of very small otic vesicles or, in severe cases, complete loss of otic tissue. Expression of *pax8* in the otic domain is not detectable in *foxi1* mutants, presumably contributing to the mutant phenotype. Conversely, misexpression of *foxi1* is sufficient to induce ectopic expression of *pax8*, suggesting that Foxi1 serves as an upstream activator of *pax8* expression. To test this predicted epistatic relationship, we co-injected *foxi1*-MO and *pax8*-MO into wild-type embryos. Knockdown of *foxi1* and *pax8* causes defects in otic development that are indistinguishable from the effects of injecting *foxi1*-MO alone (Fig. 8A–F), supporting the notion that *foxi1* and *pax8* function in a simple linear pathway.

dlx3b is another early regulator of preotic development, and mutants homozygous for a deletion that removes *dlx3b* (as well as *dlx4b* and *sox9a*) show severe deficiency of otic tissue. However, they show nearly normal expression of *pax8* (Solomon and Fritz, 2002). Furthermore, early expression of *dlx3b* along the edges of the neural plate is independent of Fgf signaling and *pax8* function (Fig. 4). These and other data strongly suggest that *pax8* and *dlx3b* are at least initially in independent pathways. To investigate the epistatic relationship between these genes, embryos were co-injected with *dlx3b*-

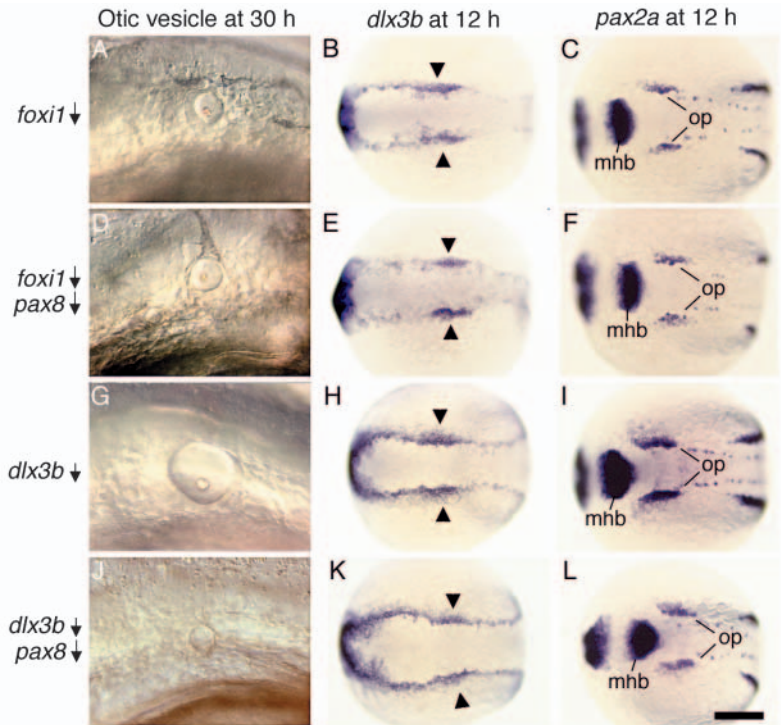


Fig. 8. *pax8* acts downstream of *foxi1* and in parallel with *dlx3b*. Wild-type embryos injected with *foxi1*-MO (A–C), *foxi1*-MO plus *pax8*-MO (D–F), *dlx3b*-MO (G–I), or *dlx3b*-MO plus *pax8*-MO (J–L). Images show lateral views of the otic vesicle at 30 hpf (A,D,G,J), or dorsal views of *dlx3b* expression at 12 hpf (B,E,H,K) and *pax2a* expression at 12 hpf (C,F,I,L). Anterior is to the left in all specimens. mhb, midbrain-hindbrain border; op, otic placode. Arrowheads mark the otic region of *dlx3b* expression. Scale bar in L: 50 μ m for A,D,G,J; 200 μ m for B,C,E,F,H,I,K,L.

MO and *pax8*-MO. In *dlx3b-pax8* double morphant embryos, preotic domains of *dlx3b* and *pax2a* are reduced relative to those seen in embryos depleted for *dlx3b* or *pax8* alone (Fig. 8H,I,K,L). Otic vesicles are dramatically reduced in size and typically produce no hair cells or otoliths (Fig. 8G,J; and data not shown), indicating severe deficiencies in otic differentiation. These findings show that *pax8* and *dlx3b* do not operate in a simple linear pathway.

Discussion

Exonic structure of *pax8*

We have completed the *pax8* cDNA sequence and identified three main variants of transcripts with several subvariants present. While most features of the exon-intron structure are conserved with mammalian *Pax8*, the zebrafish sequence shows several unique features. Most significantly, we identified three main categories of splice variants that vary in their N-terminal sequences, leading to the use of two alternative start codons. The predicted ORF for variant 1 begins ten amino acids within the canonical Paired domain and would presumably disrupt the DNA-binding ability of the N-terminal portion of this domain (Xu et al., 1995). Variants 2 and 3 encode proteins that contain the entire canonical Paired domain. The Paired domain comprises N-terminal and C-

terminal subdomains, which mediate binding to distinct parts of a conserved DNA consensus sequence. Although no isoforms using alternate start codons have been identified in the mouse or human, one mammalian isoform, Pax8(S), contains an additional serine residue in the N-terminal subdomain. This insertion functionally inactivates the N-terminal subdomain, causing Pax8(S) to bind a different DNA consensus sequence through its C-terminal subdomain, perhaps analogous to the zebrafish variant 1 vs. variant 2-3 isoforms. Pax8(S) accounts for roughly one-third of Pax8 produced in all tissues, extending the range of target genes potentially regulated by the *Pax8* locus (Kozmik et al., 1997). It is possible that the zebrafish isoform with an incomplete N-terminal subdomain has altered binding properties similar to mammalian Pax8(S). Interestingly, Fugu *pax8* also encodes a methionine at position 10 of the Paired domain (Pfeffer et al., 1998), and thus may encode a set of Pax8 proteins similar to zebrafish. Although the exact functional differences between these isoforms remain to be elucidated, our data suggest that variant 1 and variant 2/3 isoforms appear to have both overlapping and unique functions as revealed by knockdown in the *noi* (*pax2*) mutant background.

At least six splice variants found in the mouse and human show changes in C-terminal sequences (Kozmik et al., 1993), and even more C-terminal variants are found in zebrafish. Other Pax8 functional domains, including the transactivation domain and the inhibitory domain, are disrupted in these isoforms. The functional significance of C-terminal variation is presently unknown; however, altering the structure of the functional domains may create proteins with altered DNA sequence specificity or varying transactivation potentials, as has been previously reported for other members of the zebrafish and mammalian Pax gene families (Barber et al., 1999; Barr et al., 1999; Epstein et al., 1994; Kozmik et al., 1997; Kozmik et al., 1993; Nornes et al., 1996; Puschel et al., 1992; Seo et al., 1998; Tavassoli et al., 1997; Vogan et al., 1996; Zwollo et al., 1997). It should be noted that these alternatively spliced isoforms appear to be rare in zebrafish.

Redundancy among Pax2 and pax8 genes

Knockdown of *pax8* causes significant reduction in the amount of otic tissue produced during induction, and the deficit persists through subsequent stages of otic development. The small vesicle that is eventually produced expresses regional markers normally but shows deficiencies in sensory epithelia. In severe cases, various maculae or cristae are missing or fused, possibly as a nonspecific consequence of the presence of too little otic tissue. The closely related genes *pax2a* and *pax2b* are expressed at slightly later stages of preotic development and appear to partially overlap in function with *pax8*. Disruption of both *pax2a* and *pax2b* function causes only subtle defects in otic development, suggesting that *pax8* can substantially compensate for their loss. When the function of all three Pax genes is disrupted, otic tissue shows progressive diminution during placodal development and is lost entirely by 24 hpf. Staining with acridine orange does not reveal an obvious increase in otic cell death, suggesting that otic these cells eventually dedifferentiate in the absence of otic maintenance mediated by *pax2a*, *pax2b*, and *pax8*. This notion is further supported by the observation that the otic domain of *dlx3b* expression appears to be progressively lost beginning around

24 hpf. These data strongly support the hypothesis that *pax8* and *pax2* functions are partially redundant. A similar relationship among murine *Pax2/5/8* family members seems likely as well. *Pax8* and *Pax2* are expressed in the developing murine ear at the same relative stages as in zebrafish (Pfeffer et al., 1998). No ear defects have been reported in *Pax8* knockout mice (Bouchard et al., 2002; Mansouri et al., 1998), and defects in *Pax2* knockout mice are limited to disturbances in medial otic vesicle development (Bouchard et al., 2000; Burton et al., 2004; Favor et al., 1996; Torres et al., 1996). Otic development has not yet been described in *Pax8-Pax2* double knockout mice, but it seems likely that much more severe otic defects will result in such embryos. Indeed, such has been observed with respect to kidney development (Bouchard et al., 2002). The developing kidney undergoes apoptotic cell death at an early stage in *Pax8-Pax2* double mutants, a phenotype not observed in either of the single mutants (Bouchard et al., 2002).

pax8 as part of a genetic network.

Induction of *pax8* expression requires at least two distinct pathways, one mediated by *foxi1* and the other by Fgf signaling (Leger and Brand, 2002; Maroon et al., 2002; Nissen et al., 2003; Phillips et al., 2001; Solomon et al., 2003; Solomon et al., 2004). These inductive pathways are partially independent, but some aspects of *foxi1* expression appear to be regulated by Fgf signaling. *foxi1* is initially expressed in ventral ectoderm but then shows upregulation in periotic ectoderm roughly 30-60 minutes before induction of *pax8*. The spatial pattern of *foxi1* expression is unaltered in embryos depleted for Fgf3 and Fgf8 (Solomon et al., 2004), but misexpression of *Fgf3* or *Fgf8* is sufficient to induce *foxi1* expression in ectopic locations (Phillips et al., 2004). It is possible that *foxi1* is sensitive to residual Fgf signaling in *Fgf* morphants or, alternatively, Fgf3 and Fgf8 may act in concert with other factors to regulate *foxi1*. In any case, expression of *pax8* occurs in the region where *foxi1* and Fgf signaling overlap, and serves as an important nexus linking these pathways.

Our data also indicate that *pax8* positively regulates its own expression since the level of *pax8* expression is reduced in *pax8* morphants. We speculate that *pax8* helps mediate otic induction and that this feedback loop magnifies the efficacy of Fgf signaling, extending the range of Fgf action to cells farther from the source. Thus, loss of *pax8* would be expected to limit otic induction to cells in close proximity to the signaling source, a prediction borne out by our studies. Subsequent expression of *pax2a* and *pax2b*, which require Fgf signaling but not *pax8*, presumably stabilizes otic fate within the diminished population of preotic cells. Such a model could explain why eliminating *Pax8* in the mouse has such mild consequences; in the mouse, *Fgf3* is expressed directly within preotic cells, making the need for signal amplification less critical during initial stages of otic induction. Later expression of *Pax2* might then be sufficient to stabilize otic development initiated by prior Fgf signaling.

A number of other transcription factors have been implicated in early otic development, the best characterized of which are *dlx3b* and *dlx4b*. *dlx3b/4b* are initially expressed in ventral ectoderm but become restricted by 9 hpf to a contiguous line of cells surrounding the neural plate (Akimenko et al., 1994). By 11 hpf, *dlx3b/4b* show strong upregulation in preotic cells. The early phases of *dlx3b/4b* expression are independent of Fgf

signaling, but later upregulation in the otic anlagen fails to occur in embryos depleted for Fgf3 and Fgf8 (Liu et al., 2003; Solomon, 2004); (this report). As such, *dlx3b* and *dlx4b* could serve as another mediator of Fgf signaling (Solomon, 2004). Knockdown of either *dlx* gene causes mild to moderate deficiencies in otic development, with much more severe deficiencies seen in embryos knocked down for both (Liu et al., 2003; Solomon and Fritz, 2002). Embryos homozygous for a deletion that removes *dlx3b*, *dlx4b* and *sox9a* (a third preotic marker under control of Fgf signaling) fail to produce an ear, although roughly one-third of mutant embryos produce a few disorganized otic cells that belatedly express *pax2a*. This severe disruption occurs despite the fact that *pax8* is initially expressed normally (Solomon and Fritz, 2002). Thus, *pax8* is clearly not sufficient to sustain early otic development. Other transcription factors also play crucial roles during otic induction.

In this paper, we have shown that knockdown of both *pax2a* and *pax8* causes much more severe loss of ear tissue than knocking down either alone. We have previously shown that *foxi1*, which is required for *pax8* expression in the otic domain, and *dlx3b* act in parallel pathways in early otic placode formation and show a strong synergistic genetic interaction (Solomon, 2004). The *pax8-dlx3b* morphant analysis confirms these previous results and furthermore suggests that a significant aspect but not all of *foxi1* function is mediated by *pax8*. Thus, there appear to be multiple regulatory genes that respond to Fgf signaling and help mediate its effects. Each is likely to control both redundant and specific functions; hence there is neither a single 'master regulator', analogous to the role played by *pax6/eyeless* during eye development, nor an 'all-or-none' combinatorial code required for otic induction. This model partly accounts for the remarkable resilience and regulative capacity of the developing inner ear (Baker and Bronner-Fraser, 2001; Noramly and Grainger, 2002; Riley and Phillips, 2003; Torres and Giraldez, 1998). A similar series of experiments involving *pax2-pax8*, *dlx3b*, *foxi1*, *fgf3-fgf8* and *sox9* genes has been performed by Hans and colleagues (Hans et al., 2004). They propose a model that fully agrees with the findings and conclusions presented here (Hans et al., 2004), as well as the model proposed by Solomon et al. (Solomon et al., 2004).

We thank Monte Westerfield and colleagues for sharing information prior to publication. This work was supported by the National Institutes of Health, NIDCD Grant RO1-DC04701 (A.F. and M.D.M.) and the National Institutes of Health, NIDCD Grant RO1-DC03806 (B.B.R. and S.J.K.).

References

- Akimenko, M. A., Ekker, M., Wegner, J., Lin, W. and Westerfield, M. (1994). Combinatorial expression of three zebrafish genes related to distal-less: part of a homeobox gene code for the head. *J. Neurosci.* **14**, 3475-3486.
- Alvarez, Y., Alonso, M. T., Vendrell, V., Zelarayan, L. C., Chamero, P., Theil, T., Bosl, M. R., Kato, S., Maconochie, M., Riethmacher, D. et al. (2003). Requirements for FGF3 and FGF10 during inner ear formation. *Development* **130**, 6329-6338.
- Baker, C. V. and Bronner-Fraser, M. (2001). Vertebrate cranial placodes I. Embryonic induction. *Dev. Biol.* **232**, 1-61.
- Barber, T. D., Barber, M. C., Cloutier, T. E. and Friedman, T. B. (1999). PAX3 gene structure, alternative splicing and evolution. *Gene* **237**, 311-319.
- Barr, F. G., Fitzgerald, J. C., Ginsberg, J. P., Vanella, M. L., Davis, R. J. and Bencicelli, J. L. (1999). Predominant expression of alternative PAX3 and PAX7 forms in myogenic and neural tumor cell lines. *Cancer Res.* **59**, 5443-5448.
- Bouchard, M., Pfeffer, P. and Busslinger, M. (2000). Functional equivalence of the transcription factors Pax2 and Pax5 in mouse development. *Development* **127**, 3703-3713.
- Bouchard, M., Souabni, A., Mandler, M., Neubuser, A. and Busslinger, M. (2002). Nephric lineage specification by Pax2 and Pax8. *Genes Dev.* **16**, 2958-2970.
- Brand, M., Heisenberg, C. P., Jiang, Y. J., Beuchle, D., Lun, K., Furutani-Seiki, M., Granato, M., Haffter, P., Hammerschmidt, M., Kane, D. A. et al. (1996). Mutations in zebrafish genes affecting the formation of the boundary between midbrain and hindbrain. *Development* **123**, 179-190.
- Burton, Q., Cole, L. K., Mulheisen, M., Chang, W. and Wu, D. K. (2004). The role of Pax2 in mouse inner ear development. *Dev. Biol.* **272**, 161-175.
- Chi, N. and Epstein, J. A. (2002). Getting your Pax straight: Pax proteins in development and disease. *Trends Genet.* **18**, 41-47.
- Czerny, T., Bouchard, M., Kozmik, Z. and Busslinger, M. (1997). The characterization of novel Pax genes of the sea urchin and Drosophila reveal an ancient evolutionary origin of the Pax2/5/8 subfamily. *Mech. Dev.* **67**, 179-192.
- Dahl, E., Koseki, H. and Balling, R. (1997). Pax genes and organogenesis. *Bioessays* **19**, 755-765.
- Dorfler, P. and Busslinger, M. (1996). C-terminal activating and inhibitory domains determine the transactivation potential of BSAP (Pax-5), Pax-2 and Pax-8. *EMBO J.* **15**, 1971-1982.
- Draper, B. W., Morcos, P. A. and Kimmel, C. B. (2001). Inhibition of zebrafish *fgf8* pre-mRNA splicing with morpholino oligos: a quantifiable method for gene knockdown. *Genesis* **30**, 154-156.
- Ekker, M., Akimenko, M. A., Bremiller, R. and Westerfield, M. (1992a). Regional expression of three homeobox transcripts in the inner ear of zebrafish embryos. *Neuron* **9**, 27-35.
- Ekker, S. C., von Kessler, D. P. and Beachy, P. A. (1992b). Differential DNA sequence recognition is a determinant of specificity in homeotic gene action. *EMBO J.* **11**, 4059-4072.
- Ellies, D. L., Stock, D. W., Hatch, G., Giroux, G., Weiss, K. M. and Ekker, M. (1997). Relationship between the genomic organization and the overlapping embryonic expression patterns of the zebrafish *dlx* genes. *Genomics* **45**, 580-590.
- Epstein, J. A., Glaser, T., Cai, J., Jepeal, L., Walton, D. S. and Maas, R. L. (1994). Two independent and interactive DNA-binding subdomains of the Pax6 paired domain are regulated by alternative splicing. *Genes Dev.* **8**, 2022-2034.
- Favor, J., Sandulache, R., Neuhauser-Klaus, A., Pretsch, W., Chatterjee, B., Senft, E., Wurst, W., Blanquet, V., Grimes, P., Sporle, R. et al. (1996). The mouse Pax2(1Neu) mutation is identical to a human PAX2 mutation in a family with renal-coloboma syndrome and results in developmental defects of the brain, ear, eye, and kidney. *Proc. Natl. Acad. Sci. USA* **93**, 13870-13875.
- Hans, S., Liu, D. and Westerfield, M. (2004). Pax8 and Pax2a function synergistically in otic specification, downstream of the Foxi1 and Dlx3b transcription factors. *Development* **131**, 5091-5102.
- Jowett, T. (1996). Double fluorescent in situ hybridization to zebrafish embryos. *Trends Genet.* **12**, 387-389.
- Kimmel, C. B., Ballard, W. W., Kimmel, S. R., Ullmann, B. and Schilling, T. F. (1995). Stages of embryonic development of the zebrafish. *Dev. Dyn.* **203**, 253-310.
- Kozmik, Z., Kurzbauer, R., Dorfler, P. and Busslinger, M. (1993). Alternative splicing of Pax-8 gene transcripts is developmentally regulated and generates isoforms with different transactivation properties. *Mol. Cell. Biol.* **13**, 6024-6035.
- Kozmik, Z., Czerny, T. and Busslinger, M. (1997). Alternatively spliced insertions in the paired domain restrict the DNA sequence specificity of Pax6 and Pax8. *EMBO J.* **16**, 6793-6803.
- Krauss, S., Johansen, T., Korzh, V., Moens, U., Ericson, J. U. and Fjose, A. (1991). Zebrafish *pax[zf-a]*: a paired box-containing gene expressed in the neural tube. *EMBO J.* **10**, 3609-3619.
- Krelova, J., Holland, L. Z., Schubert, M., Burgtorf, C., Benes, V. and Kozmik, Z. (2002). Functional equivalency of amphioxus and vertebrate Pax258 transcription factors suggests that the activation of mid-hindbrain specific genes in vertebrates occurs via the recruitment of Pax regulatory elements. *Gene* **282**, 143-150.
- Leger, S. and Brand, M. (2002). Fgf8 and Fgf3 are required for zebrafish ear placode induction, maintenance and inner ear patterning. *Mech. Dev.* **119**, 91-108.

- Liu, D., Chu, H., Maves, L., Yan, Y. L., Morcos, P. A., Postlethwait, J. H. and Westerfield, M. (2003). Fgf3 and Fgf8 dependent and independent transcription factors are required for otic placode specification. *Development* **130**, 2213-2224.
- Lun, K. and Brand, M. (1998). A series of no isthmus alleles of the zebrafish pax2.1 gene reveals multiple signaling events in development of the midbrain-hindbrain boundary. *Development* **125**, 3049-3062.
- Mansouri, A., Hallonet, M. and Gruss, P. (1996). Pax genes and their roles in cell differentiation and development. *Curr. Opin. Cell Biol.* **8**, 851-857.
- Mansouri, A., Chowdhury, K. and Gruss, P. (1998). Follicular cells of the thyroid gland require Pax8 gene function. *Nat. Genet.* **19**, 87-90.
- Maroon, H., Walshe, J., Mahmood, R., Kiefer, P., Dickson, C. and Mason, I. (2002). Fgf3 and Fgf8 are required together for formation of the otic placode and vesicle. *Development* **129**, 2099-2108.
- Nasevicius, A. and Ekker, S. C. (2000). Effective targeted gene 'knockdown' in zebrafish. *Nat. Genet.* **26**, 216-220.
- Nissen, R. M., Yan, J., Amsterdam, A., Hopkins, N. and Burgess, S. M. (2003). Zebrafish foxi one modulates cellular responses to Fgf signaling required for the integrity of ear and jaw patterning. *Development* **130**, 2543-2554.
- Noramly, S. and Grainger, R. M. (2002). Determination of the embryonic inner ear. *J. Neurobiol.* **53**, 100-128.
- Nornes, S., Mikkola, I., Krauss, S., Delghandi, M., Perander, M. and Johansen, T. (1996). Zebrafish Pax9 encodes two proteins with distinct C-terminal transactivating domains of different potency negatively regulated by adjacent N-terminal sequences. *J. Biol. Chem.* **271**, 26914-26923.
- Oxtoby, E. and Jowett, T. (1993). Cloning of the zebrafish krox-20 gene (krox-20) and its expression during hindbrain development. *Nucleic Acids Res.* **21**, 1087-1095.
- Pfeffer, P. L., Gerster, T., Lun, K., Brand, M. and Busslinger, M. (1998). Characterization of three novel members of the zebrafish Pax2/5/8 family: dependency of Pax5 and Pax8 expression on the Pax2.1 (noi) function. *Development* **125**, 3063-3074.
- Phillips, B. T., Bolding, K. and Riley, B. B. (2001). Zebrafish fgf3 and fgf8 encode redundant functions required for otic placode induction. *Dev. Biol.* **235**, 351-365.
- Phillips, B. T., Storch, E. M., Lekven, A. C. and Riley, B. B. (2004). A direct role for Fgf but not Wnt in otic placode induction. *Development* **131**, 923-931.
- Plachov, D., Chowdhury, K., Walther, C., Simon, D., Guenet, J. L. and Gruss, P. (1990). Pax8, a murine paired box gene expressed in the developing excretory system and thyroid gland. *Development* **110**, 643-651.
- Puschel, A. W., Gruss, P. and Westerfield, M. (1992). Sequence and expression pattern of pax-6 are highly conserved between zebrafish and mice. *Development* **114**, 643-651.
- Riley, B. B. and Phillips, B. T. (2003). Ringing in the new ear: resolution of cell interactions in otic development. *Dev. Biol.* **261**, 289-312.
- Riley, B. B., Chiang, M., Farmer, L. and Heck, R. (1999). The deltaA gene of zebrafish mediates lateral inhibition of hair cells in the inner ear and is regulated by pax2.1. *Development* **126**, 5669-5678.
- Seo, H. C., Saetre, B. O., Havik, B., Ellingsen, S. and Fjose, A. (1998). The zebrafish Pax3 and Pax7 homologues are highly conserved, encode multiple isoforms and show dynamic segment-like expression in the developing brain. *Mech. Dev.* **70**, 49-63.
- Solomon, K. S. and Fritz, A. (2002). Concerted action of two dlx paralogs in sensory placode formation. *Development* **129**, 3127-3136.
- Solomon, K. S., Kudoh, T., Dawid, I. B. and Fritz, A. (2003). Zebrafish foxi1 mediates otic placode formation and jaw development. *Development* **130**, 929-940.
- Solomon, K. S., Kwak, S. J. and Fritz, A. (2004). Genetic interactions underlying otic placode induction and formation. *Dev. Dyn.* **230**, 419-433.
- Stuart, E. T., Kioussi, C. and Gruss, P. (1994). Mammalian Pax genes. *Annu. Rev. Genet.* **28**, 219-236.
- Tavassoli, K., Ruger, W. and Horst, J. (1997). Alternative splicing in PAX2 generates a new reading frame and an extended conserved coding region at the carboxy terminus. *Hum. Genet.* **101**, 371-375.
- Torres, M. and Giraldez, F. (1998). The development of the vertebrate inner ear. *Mech. Dev.* **71**, 5-21.
- Torres, M., Gomez-Pardo, E. and Gruss, P. (1996). Pax2 contributes to inner ear patterning and optic nerve trajectory. *Development* **122**, 3381-3391.
- Treisman, J., Harris, E. and Desplan, C. (1991). The paired box encodes a second DNA-binding domain in the paired homeo domain protein. *Genes Dev.* **5**, 594-604.
- Underhill, D. A. and Gros, P. (1997). The paired-domain regulates DNA binding by the homeodomain within the intact Pax-3 protein. *J. Biol. Chem.* **272**, 14175-14182.
- Vogan, K. J., Underhill, D. A. and Gros, P. (1996). An alternative splicing event in the Pax-3 paired domain identifies the linker region as a key determinant of paired domain DNA-binding activity. *Mol. Cell. Biol.* **16**, 6677-6686.
- Walther, C., Guenet, J. L., Simon, D., Deutsch, U., Jostes, B., Goulding, M. D., Plachov, D., Balling, R. and Gruss, P. (1991). Pax: a murine multigene family of paired box-containing genes. *Genomics* **11**, 424-434.
- Whitfield, T. T., Riley, B. B., Chiang, M. Y. and Phillips, B. (2002). Development of the zebrafish inner ear. *Dev. Dyn.* **223**, 427-458.
- Wiellette, E. L. and Sive, H. (2004). Early requirement for fgf8 function during hindbrain pattern formation in zebrafish. *Dev. Dyn.* **229**, 393-399.
- Wright, T. J. and Mansour, S. L. (2003). Fgf3 and Fgf10 are required for mouse otic placode induction. *Development* **130**, 3379-3390.
- Xu, W., Rould, M. A., Jun, S., Desplan, C. and Pabo, C. O. (1995). Crystal structure of a paired domain-DNA complex at 2.5 Å resolution reveals structural basis for Pax developmental mutations. *Cell* **80**, 639-650.
- Zwollo, P., Arrieta, H., Ede, K., Molinder, K., Desiderio, S. and Pollock, R. (1997). The Pax-5 gene is alternatively spliced during B-cell development. *J. Biol. Chem.* **272**, 10160-10168.